CEA EURATOM

ASSOCIATION EURATOM - C.E.A.

DEPARTEMENT DE RECHERCHES
SUR LA FUSION CONTROLEE

DRFC-SCP-STGI

EUR-CEA-FC-1198

FR8400188

TIME AND ENERGY RESOLVED RUNAWAY MEASUREMENTS IN TFR FROM INDUCED RADIOACTIVITY

TFR Group

September 1983

Submitted for publication in Nuclear Fusion

Time and Energy Resolved Runaway Measurements in TFR from Induced Radioactivity

T F R Group

ASSOCIATION EURATOM-CEA SUR LA FUSION
Département de Recherches sur la Fusion Contrôlée
Centre d'Etudes Nucléaires
Boîte Postale n°6. 92260 FONTENAY-AUX-ROSES (FRANCE)

ABSTRACT

A time and energy resolved measurement of the radioactivity induced by runaway electrons in proper samples has been developped in TFR. The data give an information on the confinement time of these electrons, which appears to be strongly dependent on the toroidal field, suggesting the onset of a magnetic turbulence at lower fields. Observations showing that the runaway electrons deeply penetrate into the limiter shadow are also reported.

It is well known that runaway electrons (RAE) may appear in Tokamaks up to energies of tens of MeV. The possibility to use such RAE to probe the magnetic field structure appears as an efficient way to check the importance of the magnetic turbulence present in the plasma. Actually, because of their large parallel velocity $\sim C$, RAE tend to integrate the transverse drifts due to fluctuating electric fields. A deviation of their confinement time with respect to the classical drift orbit effect is rather attributable to magnetic fluctuations. Several experimental techniques have been used to obtain informations on the RAE behaviour, all of them based upon the

secondary radiations emitted when RAE interact with the plasma or the limiter. Such techniques consist of the measurement of the hardX rays emitted by bremsstrahlung [1], the detection of the neutrons produced by electro - or photo - desintegration [2], and the detection of the radioactivity induced in the limiter [2,3]. The experimental results which are reported hereafter have been obtained by this last method. However a basic improvement, allowing time and energy resolution, has been achieved. Up to now radioactivity measurements were carried out by removing limiters after hundreds of shots. The conclusions on the RAE behaviour were then global. The device depicted on Fig (1 a-b) is designed to measure the radioactivity which is induced in proper samples during a controlled time interval of a single discharge. The samples are placed in a shuttle located behind a target in contact with the plasma. At any time during a discharge the shuttle may be withdrawn and moved into an area shielded against hard X rays, where the radioactivity of the samples is measured by a Ge(Li) diode. The shuttle escapes from hard X ray irradiation after about 30 ms, a relatively short time compared to the discharge duration 400-600 ms. The radioactivity induced by the RAE impinging the target may thus be measured from the beginning of the discharge (the shuttle is located behind the target at that time) up to any chosen time within the discharge duration. Of course a series of reproducible shots is necessary to obtain an information on the time evolution of the RAE in the plasma. The energy resolution is obtained by using a blend of several samples with various thresholds for reactions (γ, γ), (γ, n), $(\gamma, 2n)$. These energies are distributed between 2 and 15 MeV (see table 1). The shape of the stainless steel target in contact with the plasma (see fig. (1.b)) has been chosen so that the sample is located within the bremsstrahlung beam and the activation efficiency is maximum. The target is radially movable in order to scan the shadow of the limiter. The main

advantage of the system with respect to hard X ray spectroscopy [1] is to allow the study of the behaviour of RAE over a wider energy spectrum. On the other hand the measurements with the Ge(Li) diode are carried out after each shot on a time scale of the order of the radionuclides periods, typically >>1 s, and noise problems are alleviated.

The results which are now given were obtained for discharges with the following parameters

- Toroidal field - 30 or 40 kG.
- Plasma current - 140 kA.
- Loop voltage - 2 V.
- Mean density - 2-3 10^{13} cm^{-3}.
- Electron temperature - 1,2 - 1,5 keV.
- Discharge length - 600 ms.

At 30 or at 40 kG the density, the temperature and the loop voltage are practically the same. So are the confinement time $\tau_{th} \simeq 10$ ms of energy of thermal electrons and also the calculated production of RAE [4] during the discharge (see fig. (2)). From the measurements of the density and temperature profiles, it can be inferred that the RAE are created near the plasma centre. In the above conditions, they accelerate at a calculated rate of 1 MeV/10 ms. The energy gain is associated with an outwards shift Δ along R of the drift orbits. Classical confinement is possible up to energies $\sim$ 20-40 MeV. This corresponds to classical confinement times $\sim$ 200-400 ms.

A first type of results were obtained at 40 kG by moving radially the target within the limiter shadow. In those experiments the shuttle containing the samples was thrown back to the diode system after the plasma current fall off. When the target is moved from the carbon limiter radius towards the wall radius, the radioactivity induced in the samples (during the whole discharge) drops exponentially, with e-folding lengths between 1 (See Fig. (3))

and 5 mm, depending on the series of shots. For a given series the penetration length is independent of the threshold energy of the various samples. The size of this length clearly indicates that the penetration of RAE in the limiter shadow cannot be due to the classical shift of the drift surface. Even during the decreasing phase of the plasma current, this shift increases only by 10^{-6} cm per toroidal turn so that some 10^5 turns would be necessary to achieve variations of Δ of order of millimeters. Such numbers are much larger than allowed before interception of RAE. In fact radial shifts $\sim 10^{-2} - 10^{-1}$ cm per toroidal turn are necessary to explain the observed penetrations. They could be caused by large scale tearing perturbations $\delta B_r \sim 1 - 5$ gauss at the plasma edge. Such values are indeed detected by Mirnov probes at the end of the discharges.

The main observations were carried out by sending the samples back to the diode at different times during the discharge, for the two values of the toroidal field 30 and 40 kG. The figures (4 a-b) give for these two fields the activation of various samples versus withdrawal time. The most interesting result is the following difference :

- At 40 kG the time behaviour of the activation is the same whatever the threshold energy of the sample. This activation takes place at the end of the discharge.
- At 30 kG the low threshold sample (Y^{89}, 2 MeV) is activated at early times during the discharge, whereas the high threshold samples (Zr, 12 MeV and Nd, 9.8 MeV) are activated only at the end, as in the 40 kG case.

This difference is obviously linked to the confinement of RAE. At 40 kG the synchroneous activation of various samples at the end of the discharge suggests that the RAE after they have been produced in the central zone of the plasma, are not much affected by turbulent diffusion. Therefore, they reach the target mainly because of the classical shift Δ of their drift surface, i.e., after

being accelerated during several 100 ms, up to energies largely beyond the sample threshold energies. The activation of the samples then takes place at the same time whatever the threshold energy. On the contrary at 30 kG the activation of the sample (Y^{89}, 2 MeV) takes place typically 200 ms before that of (Zr^{90}, 12 MeV) and (Nd^{142}, 9.8 MeV). We must admit that in that case the RAE reach the target by turbulent diffusion : only a small fraction are accelerated at energies E $\gtrsim$ 10 MeV, that is to say during a time > 100 ms (taking into account that dE/dt = 100 Kev/ms). Finally the experimental results suggest that the RAE experience quasi classical diffusion for a magnetic field of 40 kG, with a confinement time $\tau_R \sim$ 200 - 400 ms., whereas a turbulent behaviour, with $\tau_R <$ 100 ms, may be inferred for 30 kG. Let us recall however that the thermal electrons have the same confinement time τ_{th} = 10 ms in both cases.

To get a more precise picture we have used a simulation code [5] computing the production of RAE from the measured values of density, temperature and voltage and giving the evolution of their destribution in energy according to various assumptions on confinement. This code is associated with another code computing the radioactivity induced by the bremsstrahlung photons in the samples. At 40 kG a correct simulation is obtained by assuming classical confinement times = 200-400 ms. Of course this does not exclude a small diffusion process corresponding to a confinement time τ_R in excess of 200-400 ms. But at 30 kG, the simulation of activation of (Y^{89}, 2 MeV) necessitates to take a confinement time due to turbulent diffusion = 20-40 ms. However, such low confinement times do not allow to keep enough RAE in the plasma to justify the observed activations at higher thresholds 9.8 MeV, ... A best fit is obtained by taking the turbulent confinement τ_R increasing with energy, for instance

$$\tau_R \sim \tau_o \quad \text{for } E < E_o$$
$$\tau_R \sim \tau_o \frac{E}{E_o} \quad \text{for } E \geq E_o$$

with $\tau_o \sim$ 20-40 ms, and E_o between 1 and 10 MeV. The simulations then also agree with the measured flux of photoneutrons shown on figure (2) representative of RAE impinging on the target at energies $\geq$ 10 MeV. The figures (5 a-b) give the calculated energy distribution of the RAE reaching the target.

The difference of confinement of low energy RAE at 40 and 30 kG suggests that the magnetic component of the turbulence to which RAE are specially sensitive, is much more important at 30 kG. However the confinement of the thermal electrons is the same. Therefore, this suggests that, at least in our operating conditions, the thermal electrons should mainly diffuse under the influence of the electrostatic component of the turbulence. One may try to make a more quantitative statement by writing the turbulent electromagnetic perturbations δE, δB as :

$$\delta E = -\frac{1}{c}\frac{\partial \delta A}{\partial t} - \nabla \delta\varphi \; ; \quad \delta B = \nabla \times \delta A$$

where the electric and magnetic potentials $\delta\varphi$ and $\delta A = \delta A_{//}$ consist of modes $\sim \exp i(\ell\theta + m\varphi)$ localized (with even parity) near the resonant magnetic surfaces $m + \ell/q_{s=o}$ within a small radial distance $\delta \sim (\kappa_\theta)^{-1}$, $\kappa_\theta \sim \ell/r$. An order of magnitude of the diffusion coefficient for thermal electrons (velocity V_{th}) is obtained from the quasilinear theory [6,7] applied to circulating electrons

$$D_{th} = D_{thM} + D_{thE}$$

where

$$D_{thM} \sim \left|\frac{\delta A}{B}\right|^2 \kappa_\theta^2 \frac{V_{th}}{\kappa_{//}}$$

$$D_{thE} \sim \left|\frac{\delta\varphi}{B}\right|^2 \kappa_\theta^2 \frac{c^2}{\kappa_{//} V_{th}}$$

and $\kappa_{//} \sim \delta \cdot \kappa_\theta / \alpha_s$, $\alpha_s^{-1} = r\,\partial q / q^2 R\,\partial r$.

To simplify we have ignored shaping factors which should

be introduced in these expressions. The estimation (2) applies also to the diffusion coefficients D_{RM} and D_{RE} of RAE due to the magnetic and electric turbulence, except that V_{th} must be replaced by the RAE parallel velocity $\sim C$. On the other hand, one must take account of the reduction of the coupling between the turbulent modes and the RAE when their energy E increases and the shift Δ between the drift surfaces and the magnetic surfaces takes values larger than the radial range δ of each turbulent mode [8,9]. For $\Delta \ll r$ this effect roughly multiplies the diffusion coefficients by the usual coefficient $|J_0(K_\perp \Delta)|^2$ where $K_\perp \sim 1/\delta \sim K_\theta$. For values of $K_\perp \sim 5\ cm^{-1}$ (compatible with microwave or IR Laser beam scattering experiments) this $|J_0|^2$ factor keeps a constant value ~ 1 up to energies $E \sim 1$ MeV, and then decreases as 1/E. This is compatible with confinement times for RAE of the form (1), taking $E_0 \sim 1$ MeV, and

$$\frac{1}{\tau_0} \sim \frac{1}{r^2}\left(D_{RM} + D_{RE}\right) \sim \frac{1}{r^2}\left(D_{thE}\frac{V_{th}}{c} + D_{thM}\frac{c}{V_{th}}\right)$$

The ratio τ_0/τ_{th} where $\tau_{th} \sim r^2/(D_{thE}+D_{thM}) \sim 10$ ms is the energy confinement time of the thermal electrons then scales as

$$\frac{\tau_0}{\tau_{th}} \sim \frac{V_{th}}{c}\ \frac{D_{thM}/D_{thE}+1}{D_{thM}/D_{thE}+(V_{th}/c)^2}$$

At 40 kG, large values of $\tau_0 > 100$ms are observed. As $\tau_{th} \sim 10$ ms, the ratio τ_0/τ_{th} is in fact of the order of $C/V_{th} \sim 10$. This implies very small values of $D_{thM}/D_{thE} \sim (V_{th}/c)^2 \sim 10^{-2}$. At 30 kG smaller values of $\tau_0 \sim 20$-40 ms and of the ratio τ_0/τ_{th} must be used. This corresponds to larger values of D_{thM}/D_{thE}. However experimental data imply $\tau_0/\tau_{th} \gtrsim 1$, which forbids values of $D_{thM}/D_{thE} > V_{th}/c \sim 10^{-1}$. These estimates meet the intuitive statement made above, namely, the reported observations, while

revealing a definite level of magnetic turbulence at 30 KG , strongly suggest that, in our operating conditions, this turbulence is not responsible for the diffusion of thermal electrons. This contradicts the conclusions given for instance in [10] or [11] . Further experimentation would be welcome to clarify this point.

References

| 1 | S. Sesnic, G. Fussmann, Report IPP III/29 (1976)

| 2 | TFR group in 8th European Conference on Controlled Fusion and Plasma Physics (Prague), 1 (1977), 1

| 3 | C.W. Barnes, J.M. Stavely Jr, J.D. Strachan report PPPL 1794 (1981)

| 4 | J.W. Connor and R.J. Hastie Nucl. Fusion 15 (1975) 415

| 5 | M. Altmann, Thèse d'Etat N° 2642 (1982), Université d'Orsay, France

| 6 | A.B. Rechester and N.M. Rosenbluth, Phys. Rev. Lett. 40 (1978) 1

| 7 | F. Koechlin and A. Samain, Nuclear Fusion 18 (1978) 1509

| 8 | H.E. Mynick and J.A. Kronnes, Phys. Rev. Lett. 43 (1979) 1506

| 9 | H.E. Mynick and J.D. Strachan, Phys. Fluids 24 (1981) 695

|10 | C.W. Barnes, J.D. Strachan, Nuclear Fusion 22 (1982) 1090

|11 | K. Molvig, J.E. Rice and H.S. Tekula , Phys. Rev. Lett. 41 (1978) 1240.

Figure Captions

Table 1 - Basic properties of the samples used in the activation experiment.

Figure 1 - a. Pneumatic transport system for the samples
b. Relative toroidal positions of the target and carbon limiter.

Figure 2 - Discharge current, photoneutron emission and calculated creation rate of RAE at 40 kG (1) and 30 kG (2)

Figure 3 - Runaway electron distribution in the shadow of the carbon limiter in a case of penetration over a radial distance $\sim$ 1 mm.

Figure 4 - Time evolution of the radioactivity for several samples.
a - at 40 kG
b - at 30 kG

Figure 5 - Spectra of runaway electrons which hitted the target before several withdrawal times at 30 kG (τ_{ED} = 20ms) and at 40 kG (τ_{ED} = 200ms).

Isotope	Compound	Abundance	Reaction	Threshold (Mev)	Period (s)	Gamma energy (kev)
Y^{89}	Y_2O_3	79%	(γ,γ') Y^{89m}	$\simeq$ 2	16	910 (100%)
A^{197}	Au	100%	(γ,γ') Au^{197m}	$\simeq$ 2	7.2	280 (72%)
Pb^{208}	Pb	52%	(γ,n) Pb^{207m}	7.35	8	570 (98%)
Mo^{98}	Mo	24%	(γ,p) Nb^{97}	9.80	54	747 (100%)
Nd^{142}	Nd_2O_3	23%	(γ,n) Nd^{141m}	9.81	64	755 (100%)
Zr^{90}	Zr	52%	(γ,n) Zr^{89m}	12	252	588 (87%)
Mo^{92}	Mo	16%	(γ,n) Mo^{91m}	12.7	65	658 (48%)
Au^{107}	Au	100%	$(\gamma,2n)$ Au^{195m}	14.7	31	261 (67%)

LISTE N° 9 - Mise à jour le 4 octobre 1982

EXPLOITATION PHYSIQUE DE L'EXPERIENCE

Coordination	J. TACHON M. CHATELIER
Secrétariat scientifique	P. LECOUSTEY
Conduite de la machine	B. BEAUMONT J.M. BOTTEREAU M. CHATELIER M. DUBOIS P. GIOVANONNI L. LAURENT
Circuit poloïdal, asservissement	J. BLUM J.M. BOTTEREAU P. GIOVANONNI
Mesures magnétiques	J.L. DURANCEAU P. LECOUSTEY
Interférométrie HCN	J.P. CRENN D. VERON
Réflectométrie	R. CANO F. SIMONET
Diffusion Thomson	J. LASALLE P. PLATZ
Spectre de neu*	J.P. GIRARD T. HUTTER C. REVERDIN

Mesures neutroniques, X-durs	M. CHATELIER A. GERAUD G. MARTIN
Rayons X-mous	D. MARTY A.L. PECQUET
Spectrométrie (visible, UV, X-mous)	F. BOMBARDA C. BRETON A. COMPANT LA FONTAINE C. DE MICHELIS W. HECQ M. MATTIOLI P. PLATZ J. RAMETTE
Bolométrie	M.H. ACHARD
Spectrométrie de masse, conditionnement des parois, plasma périphérique	M.H. ACHARD P. DESCHAMPS A. GROSMAN B. TERREAULT
Rayonnement cyclotronique électronique	
a) Spectrométrie infrarouge	D. BARTLETT L. LAURENT M. TALVARD
b) Etudes microondes	R. CANO S. NOVACK B. ZANFAGNA
Mesure de la turbulence par diffusion d'ondes	B. DE GENTILE F. GERVAIS J. OLIVAIN A. QUEMENEUR L. PIGNOL N. IWAMA

Injection de glacons	D. MARTY O. LAZARE

CHAUFFAGES ADDITIONNELS

Injection de neutres	J.F. BONNAL J.M. BOTTEREAU J. DRUAUX M. FOIS J.P. GIRARD R. OBERSON J.P. ROUBIN
Chauffage cyclotronique	J. ADAM P. BANNELIER B. BEAUMONT A. BRESSON R. BRUGNETTI A. FISSOLO D. GAMBIER H. KUUS K. TEILHABER

INFORMATIQUE

Matériel	J. IOMTAL
Logiciel	J. BRETON A. COHEN J. TOUCHE
Théorie	J. ANDREOLETTI H. CAPES M. COTSAFTIS M. DUBOIS R. GRAVIER J. JOHNER E. MASCHKE C. MERCIER A. SAMAIN

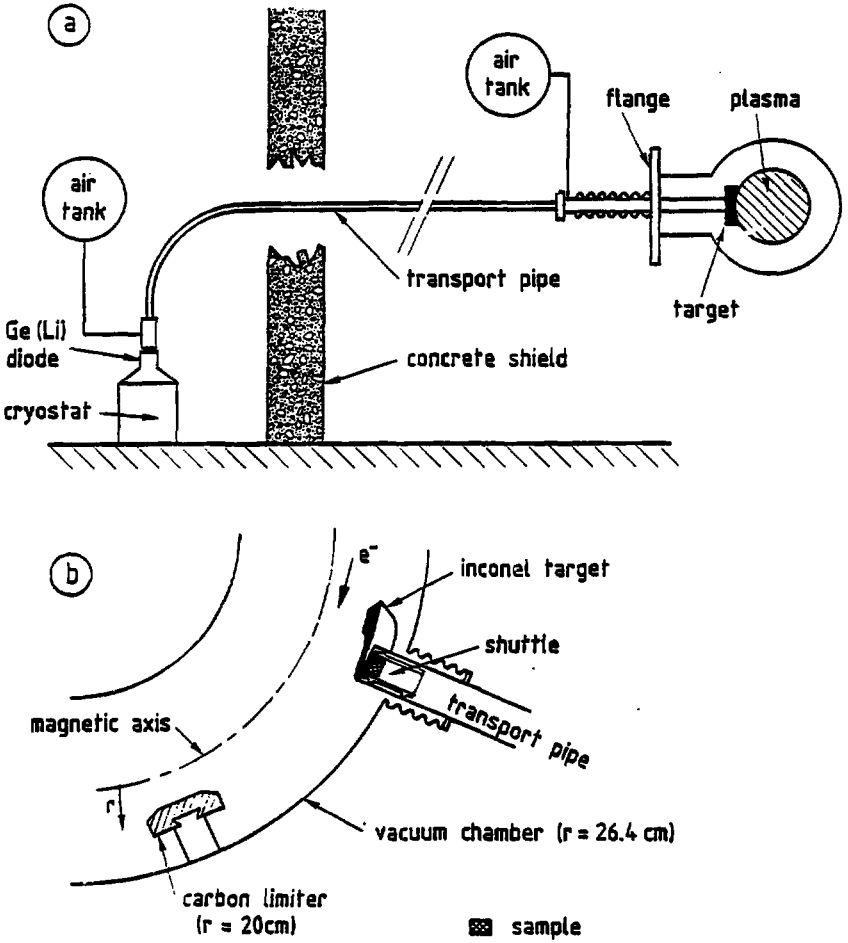
a
air tank
air tank
flange
plasma
transport pipe
target
Ge (Li) diode
concrete shield
cryostat
b
e⁻
inconel target
shuttle
magnetic axis
transport pipe
r
vacuum chamber (r = 26.4 cm)
carbon limiter (r = 20cm)
sample

Fig. 1

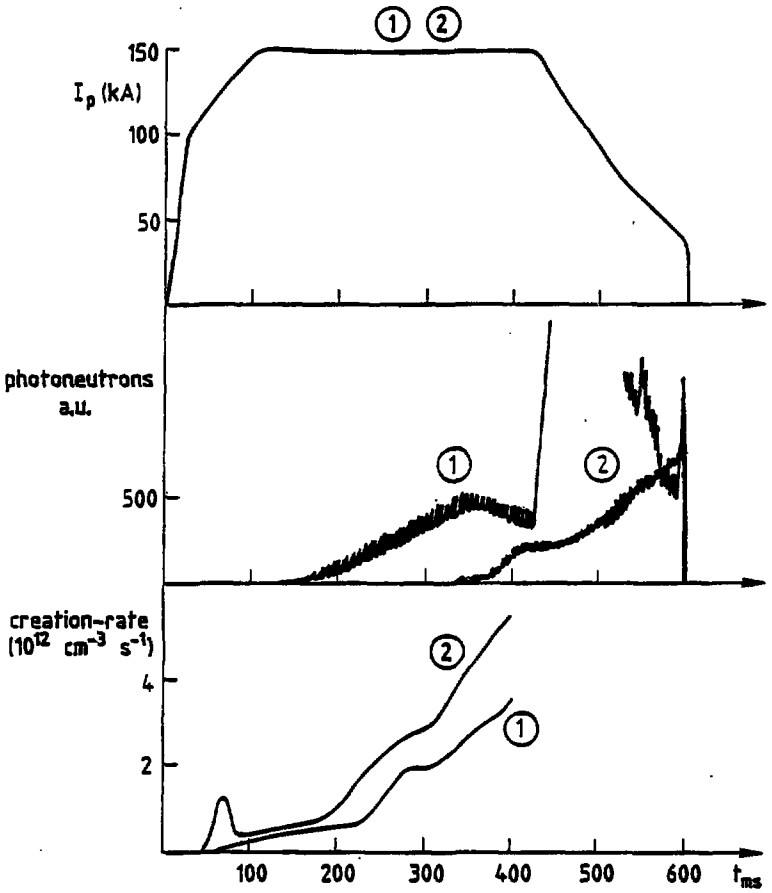
1 2
150
I_p (kA)
100
50
photoneutrons
a.u.
500
1
2
creation-rate
(10^{12} cm^{-3} s^{-1})
4
2
2
1
100
200
300
400
500
600
t_{ms}

Fig. 2

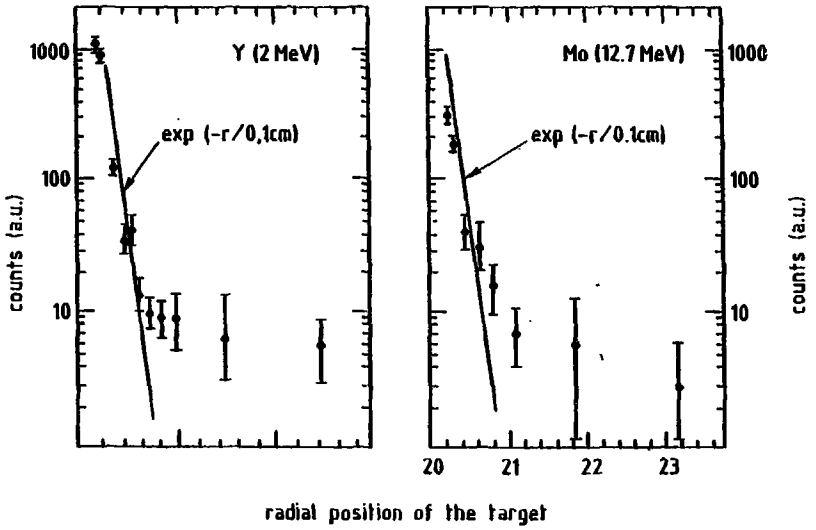
Y (2 MeV)
exp (-r/0,1cm)
Mo (12.7 MeV)
exp (-r/0.1cm)
1000
100
10
counts (a.u.)
20
21
22
23
radial position of the target

Fig. 3

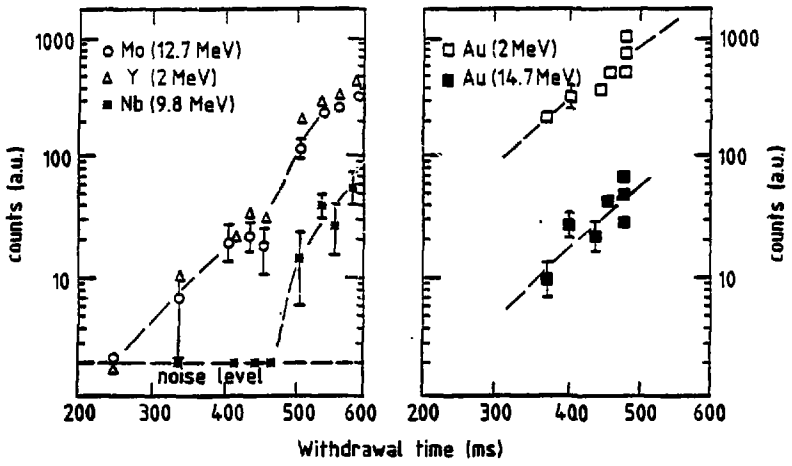

(a) - 40 kG

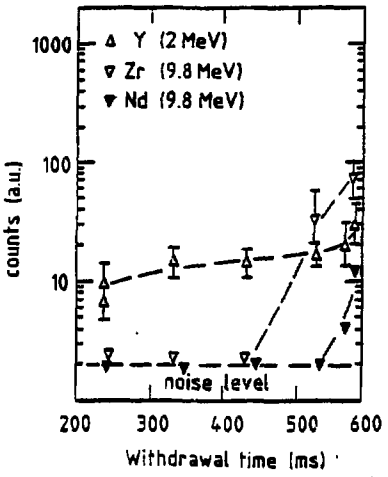

(b) - 30 kG

Fig. 4

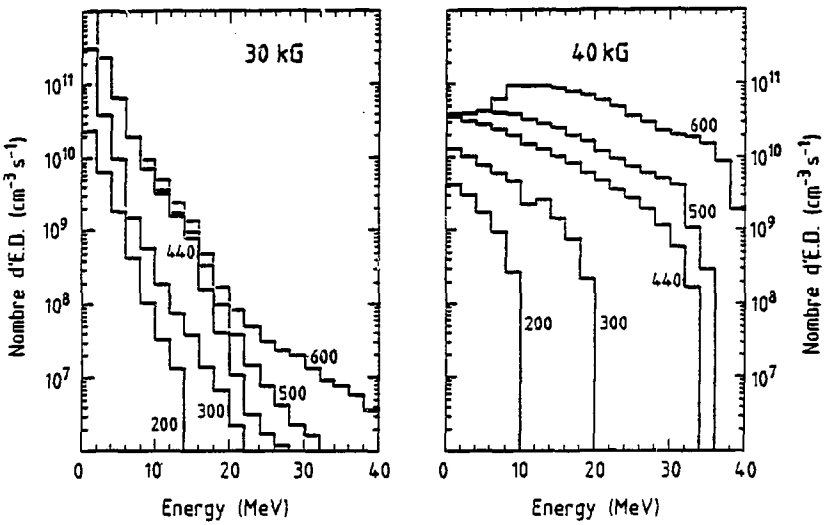

Fig. 5